AIMS Mathematics, 10(6): 13409–13431
DOI: 10.3934/math.2025602
Received: 02 April 2025
Revised: 23 May 2025
Accepted: 04 June 2025
Published: 11 June 2025

https://www.aimspress.com/journal/Math

Research article

Local bifurcation analysis of an accelerating beam subjected to two frequency parametric excitations

Fengxian An[1,3] **and Liangqiang Zhou**[2,3]*

[1] Faculty of Mathematics and Physics, Huaiyin Institute of Technology, Huaian 223003, China
[2] School of Mathematics, Nanjing University of Aeronautics and Astronautics, Nanjing 210016, China
[3] Key Laboratory of Mathematical Modelling and High Performance Computing of Air Vehicles (NUAA), MIIT, Nanjing 211106, China

* **Correspondence:** Email: zlqrex@sina.com.

Abstract: Stability and bifurcation behaviors of an axially moving beam subjected to two frequency excitations were investigated both analytically and numerically. Simultaneous principal parametric resonance as well as combination parametric resonance with 3:1 internal resonance was considered. The critical points are classified into the following categories: a double zero accompanied by two negative eigenvalues, a simple zero coexisting with a pair of pure imaginary eigenvalues, and two pairs of pure imaginary eigenvalues in the non-resonant case. Based on the normal form theory, the stability regions of the initial equilibrium point were studied and the explicit expressions of the critical bifurcation curves for the occurrence of static bifurcation and Hopf bifurcation were obtained. The critical line from which a two-dimensional torus can arise was also discussed. Moreover, numerical simulations were given, which exhibit strong concordance with the analytical predictions. The analytical results obtained here contribute to a better comprehension of the dynamical behaviors of the system and may be helpful to researchers attempting to design the system parameters of related engineering structures.

Keywords: stability; bifurcation; normal form; uniform horizontal beam
Mathematics Subject Classification: 70K20, 70K50

1. Introduction

Axially moving systems are commonly observed in many engineering applications such as paper sheets, textile fibers, robot arms, magnetic tapes, conveyor belts, band saw blades, and aerial cable tramways. These components can be modeled as axially moving strings, beams, and plates [1–3].

One important problem in axially moving mechanical systems is the abrupt occurrence of instability. Consequently, it is essential to investigate the stability characteristics and bifurcation behaviors in axially moving dynamical systems for the design of the system parameters.

Extensive research has been conducted on the nonlinear dynamical behaviors of beams. As an example of early studies, stability and bifurcation phenomenon of a shallow curved beam were discussed by Öz and Pakdemirli [4], in which the multiple scales method was employed and two-to-one internal resonance conditions between arbitrary pairs of vibration modes were studied. Applying the differential transform method, Ozgumus and Kaya [5, 6] conducted a comprehensive vibration analysis of both the doubly tapered Euler-Bernoulli beam and rotating tapered Timoshenko beam. Recently, a sufficient condition for exponential stability was established by Apalara et al. [7], depending on the equality of wave velocities within the system. In addition, the stability and vibration behaviors of axially moving beams have also been investigated by some researchers. Sze et al. [8] formulated the incremental harmonic balance method to analyze the nonlinear vibration of an axially moving beam with internal resonance between the first two transverse modes. Employing the Galerkin method, Yang and Chen [9] investigated the bifurcation phenomena and chaotic behaviors of an axially accelerating viscoelastic beam constituted by the Kelvin-Voigt model. The nonlinear dynamical behaviors were systematically studied through numerical analysis employing the Poincare map, the phase portrait, and computation of the largest Lyapunov exponent. An and Su [10] utilized the generalized integral transform technique to investigate the dynamic response of clamped axially moving beams. Comparative analysis of the vibration displacement at multiple longitudinal positions along the beam revealed excellent convergence behaviors. Later, Rajasekaran [11] adopted the differential transformation-based dynamic stiffness method to analyze the buckling and vibration behaviors of axially functionally graded tapered Euler and Timoshenko beams with different boundary conditions. Zhang et al. [12] used the Fourier expansion-based differential quadrature method to investigate the transverse nonlinear vibrations of an axially accelerating viscoelastic beam. Yan et al. [13] applied the Galerkin method to investigate the steady-state periodic response and the bifurcation and chaos of an axially accelerating viscoelastic Timoshenko beam with parametric excitation. Tang et al. [14] investigated the nonlinear steady-state oscillating response, stability, and bifurcation behaviors of a simply supported moving beam. The method of multiple scales was directly used to derive the solvability conditions, and the coupled effects of viscoelastic and viscous damping parameters on the dynamical behaviors were analyzed in detail. Recently, the stability and nonlinear vibration characteristics of axially moving beams have also been considered in a series of papers [15–18].

2. Related work

In [19], Sahoo et al. analyzed the nonlinear transverse vibration of an axially moving beam subjected to two frequency excitations by means of the multiple scales method. The frequency response plots and amplitude curves were obtained and the stability and bifurcation phenomenon were evaluated using a continuation algorithm. Numerical results were presented to show the complex nonlinear phenomena of the axially moving beam. However, the local dynamical behaviors of this system have not been studied analytically. In addition, there exist only few studies concerned with the stability and bifurcation of axially moving beams. In order to effectively suppress or eliminate large

nonlinear vibrations of axially moving beams, it is imperative to advance the theoretical analysis on axially moving beam models, analyze the complex dynamical behaviors, explore the stability regions of the initial equilibrium point, investigate the bifurcation curves for the occurrence of static bifurcation and Hopf bifurcation, and conduct comprehensive research on the impact of key system parameters, so as to ensure the stability and controllability of the axially moving beams. The present work is therefore motivated to examine stability and bifurcation behaviors of the axially moving beam considered by Sahoo et al. [19]. In this paper, both analytical and numerical methods are employed to investigate the stability and bifurcation behaviors of the axially moving beam. Simultaneous principal parametric resonance as well as combination parametric resonance with 3:1 internal resonance is considered. According to the types of the degenerated equilibrium points, three different situations will be discussed and analyzed in detail. The normal forms of the differential equations are obtained by using the symbolic computation language Maple. The approach combines the normal form theory and center manifold theory into one step to achieve the closed-form expressions. Stability conditions for the steady state solutions and transition curves are also derived by using the normal form theory and the stability and bifurcation theory. Furthermore, numerical solutions are presented, which confirm the analytical predictions.

This paper is divided as follows: In Section 3, the equations of motion for an axially moving beam subjected to two frequency excitations are given, and the stability conditions for the steady state solutions are established explicitly. A detailed study of the dynamical behaviors of the system is carried out in Section 4. Conclusions are drawn in Section 5.

3. Formulations of the problem

This paper is concerned with the nonlinear dynamical behaviors of a uniform horizontal beam traveling with a harmonically varying velocity. The model is illustrated in Figure 1 [19].

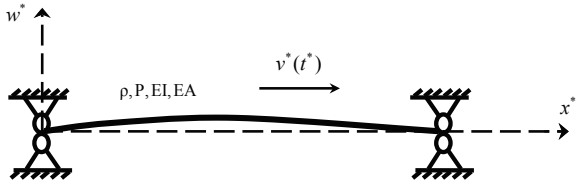

Figure 1. An axially traveling beam with variable velocity.

The nonlinear integro-partial differential equation of the beam is provided as follows [19]:

$$EI\frac{\partial^4 w^*}{\partial x^{*4}} + E^* I\frac{\partial^5 w^*}{\partial x^{*4}\partial t^*} + m\left(\frac{\partial^2 w^*}{\partial t^{*2}} + 2v^*\frac{\partial^2 w^*}{\partial x^*\partial t^*} + \frac{\partial v^*}{\partial t^*}\frac{\partial w^*}{\partial x^*} + v^{*2}\frac{\partial^2 w^*}{\partial x^{*2}}\right) - p\frac{\partial^2 w^*}{\partial x^{*2}} + c\frac{\partial w^*}{\partial t^*}$$
$$= \frac{EA}{2L}\frac{\partial^2 w^*}{\partial x^{*2}}\int_0^L \left(\frac{\partial w^*}{\partial x^*}\right)^2 \mathrm{d}x^*, \tag{3.1}$$

and the associated boundary conditions are

$$w^*(0,t^*) = w^*(L,t^*) = \frac{\partial^2 w^*}{\partial x^{*2}}(0,t^*) = \frac{\partial^2 w^*}{\partial x^{*2}}(L,t^*) = 0. \tag{3.2}$$

See [19] for the explanation of all system parameters.

3.1. Assumptions and parameters

The time dependent velocity is supposed in the following form:

$$v^* = v_0^*(1 + \eta_1 \sin \Omega_1^* t^* + \eta_2 \sin \Omega_2^* t^*), \tag{3.3}$$

where v_0^*, $v_0^* \eta_n \, (n = 1, 2)$ and $\Omega_n^* \, (n = 1, 2)$ stand for the mean velocity, the amplitudes, and the frequencies of the harmonically varying velocity components, respectively.

The following are the non-dimensional transformations of the variables and parameters:

$$\begin{aligned} &x = \frac{x^*}{L}, \; t = t^* \sqrt{\frac{P}{\rho A L^2}}, \; w = \frac{w^*}{L}, \; v = \frac{v^*}{\sqrt{P/\rho A}}, \; \alpha = \frac{IE^*}{2\varepsilon L^3 \sqrt{\rho A P}}, \\ &\mu = \frac{cL}{2\varepsilon \sqrt{\rho A P}}, \; v_l = \sqrt{\frac{EA}{P}}, \; v_f = \sqrt{\frac{EI}{PL^2}}, \; \Omega = \Omega^* \sqrt{\frac{\rho A L^2}{P}}, \end{aligned} \tag{3.4}$$

and the equation of motion of the beam in non-dimensional form is obtained as [19]

$$\ddot{w} + 2v\dot{w}' + \dot{v}w' + (v^2 - 1)w'' + v_f^2 w'''' + 2\varepsilon\alpha\dot{w}'''' + 2\varepsilon\mu\dot{w} = \frac{1}{2} v_l^2 w'' \int_0^1 w'^2 \mathrm{d}x \tag{3.5}$$

with the associated boundary conditions

$$w(0, t) = w(1, t) = w''(0, t) = w''(1, t) = 0, \tag{3.6}$$

where v_f and v_l mean the non-dimensional flexural stiffness and the non-dimensional longitudinal stiffness of the beam. μ and α represent coefficients of the non-dimensional viscous (external) damping and the non-dimensional material (internal) damping, respectively.

In order to derive the governing equations of motion, the following assumptions of the parameters and variables are introduced: (1) $v_0 \eta_n = \varepsilon v_n \, (n = 1, 2)$; (2) for the case of a small amplitude of motion, $w = \sqrt{\varepsilon} w^{\#}$, where $\varepsilon \ll 1$; (3) simultaneous principal parametric resonance of the first mode ($\Omega_1 \approx 2\omega_1$) and combination parametric resonance of the first two modes ($\Omega_2 \approx \omega_1 + \omega_2$) with 3:1 internal resonance ($\omega_2 \approx 3\omega_1$) are considered. It is supposed that the responses in higher modes die down owing to the presence of damping and the Coriolis term in the equation of motion. Therefore, the first two modes will result in the long term system response. In this case, the relations are: $\Omega_1 \approx 2\omega_1$, $\Omega_2 \approx \omega_1 + \omega_2$, and $\omega_2 \approx 3\omega_1$.

3.2. Method of analysis

Based on the aforementioned assumptions, the axial speed is obtained as

$$v = v_0 + \varepsilon v_1 \sin \Omega_1 t + \varepsilon v_2 \sin \Omega_2 t. \tag{3.7}$$

Removing the superscript "#" for convenience leads to the weakly nonlinear equation as [19]

$$\ddot{w} + 2v\dot{w}' + \dot{v}w' + (v^2 - 1)w'' + v_f^2 w'''' + 2\varepsilon\alpha\dot{w}'''' + 2\varepsilon\mu\dot{w} = \frac{1}{2} \varepsilon v_l^2 w'' \int_0^1 w'^2 \mathrm{d}x. \tag{3.8}$$

Putting Eq (3.7) into Eq (3.8), the equation of motion can be obtained as follows:

$$\ddot{w} + 2(v_0 + \varepsilon v_1 \sin\Omega_1 t + \varepsilon v_2 \sin\Omega_2 t)\dot{w}' + (\varepsilon v_1\Omega_1 \cos\Omega_1 t + \varepsilon v_2\Omega_2 \cos\Omega_2 t)w' + [(v_0 + \varepsilon v_1 \sin\Omega_1 t + \varepsilon v_2 \sin\Omega_2 t)^2 - 1]w'' + v_f^2 w'''' + 2\varepsilon\alpha\dot{w}'''' + 2\varepsilon\mu\dot{w} = \frac{1}{2}\varepsilon v_l^2 w'' \int_0^1 w'^2 \mathrm{d}x, \tag{3.9}$$

and the boundary conditions are

$$w(0,t) = w(1,t) = w''(0,t) = w''(1,t) = 0. \tag{3.10}$$

Applying the multiple scales method, the following expression can be obtained:

$$w(x,t,\varepsilon) = w_0(x,T_0,T_1) + \varepsilon w_1(x,T_0,T_1) + \cdots, \tag{3.11}$$

where $T_0 = t$, $T_1 = \varepsilon t$. Denoting the differential operators as

$$D_0 = \frac{\partial}{\partial T_0} \; and \; D_1 = \frac{\partial}{\partial T_1}$$

leads to the following expression:

$$\frac{\partial}{\partial t} = D_0 + \varepsilon D_1 + \cdots, \; \frac{\partial^2}{\partial t^2} = D_0^2 + 2\varepsilon D_0 D_1 + \cdots. \tag{3.12}$$

Substituting Eqs (3.11) and (3.12) into Eqs (3.9) and (3.10), the following equations can be obtained:

$$\begin{aligned} &D_0^2 w_0 + 2v_0 D_0 w_0' + (v_0^2 - 1)w_0'' + v_f^2 w_0'''' = 0, \\ &w_0(0,t) = w_0(1,t) = w_0''(0,t) = w_0''(1,t) = 0, \end{aligned} \tag{3.13}$$

$$\begin{aligned} &D_0^2 w_1 + 2v_0 D_0 w_1' + (v_0^2 - 1)w_1'' + v_f^2 w_1'''' = -2D_0 D_1 w_0 - 2\alpha D_0 w_0'''' \\ &- 2\mu D_0 w_0 - 2v_0 D_1 w_0' - 2(v_1 \sin\Omega_1 t + v_2 \sin\Omega_2 t)D_0 w_0' - (v_1\Omega_1 \cos\Omega_1 t \\ &+ v_2\Omega_2 \cos\Omega_2 t)w_0' - 2v_0(v_1 \sin\Omega_1 t + v_2 \sin\Omega_2 t)w_0'' + \frac{1}{2}v_l^2 w_0'' \int_0^1 w_0'^2 \mathrm{d}x, \\ &w_1(0,t) = w_1(1,t) = w_1''(0,t) = w_1''(1,t) = 0. \end{aligned} \tag{3.14}$$

The solution of Eq (3.13) can be written as

$$w_0(x,T_0,T_1) = \sum_{n=1}^{\infty} \phi_n(x) A_n(T_1) e^{i\omega_n T_0} + cc, \tag{3.15}$$

where ϕ_n means the complex mode shapes, ω_n denotes the natural frequencies, and cc is the complex conjugate.

In addition, Eq (3.15) can be replaced with

$$w_0(x,T_0,T_1) = A_1(T_1)\phi_1(x)e^{i\omega_1 T_0} + A_2(T_1)\phi_2(x)e^{i\omega_2 T_0}. \tag{3.16}$$

The frequency detuning parameters σ_1, σ_2, and σ_3 are introduced with the following relations:

$$\omega_2 = 3\omega_1 + \varepsilon\sigma_1,\ \Omega_1 = 2\omega_1 + \varepsilon\sigma_2,\ \Omega_2 = \omega_1 + \omega_2 + \varepsilon\sigma_3. \tag{3.17}$$

Substituting Eqs (3.14) and (3.15) into Eq (3.9), two complex variable modulation equations are obtained as follows [19]:

$$\begin{aligned} &2\dot{A}_1 + 8s_1A_1^2\bar{A}_1 + 8s_2A_1A_2\bar{A}_2 + 8g_1\bar{A}_1^2A_2e^{i\sigma_1T_1} + 2\mu C_1A_1 + 2\alpha e_1A_1 \\ &+ 2K_1\bar{A}_1e^{i\sigma_2T_1} + 2K_2A_2e^{i(\sigma_1-\sigma_2)T_1} + 2K_8\bar{A}_2e^{i\sigma_3T_1} = 0, \end{aligned} \tag{3.18a}$$

$$\begin{aligned} &2\dot{A}_2 + 8s_4A_2^2\bar{A}_2 + 8s_3A_1A_2\bar{A}_1 + 8g_2A_1^3e^{-i\sigma_1T_1} + 2\mu C_2A_2 \\ &+ 2\alpha e_2A_2 + 2K_3A_1e^{i(\sigma_2-\sigma_1)T_1} + 2K_9\bar{A}_1e^{i\sigma_3T_1} = 0, \end{aligned} \tag{3.18b}$$

where the dot denotes the differentiation with respect to T_1, and s_i, g_i, K_i, C_i, and e_i are nonlinear interaction coefficients. The over bar signifies a complex conjugate.

Employing the Cartesian transformation for A_n $(n = 1, 2)$, we have

$$A_1(T_1) = \frac{1}{2}[x_1(T_1) - ix_2(T_1)]e^{i\lambda_1T_1}, \quad A_2(T_1) = \frac{1}{2}[x_3(T_1) - ix_4(T_1)]e^{i\lambda_2T_1}, \tag{3.19}$$

where x_i (T_1) $(i = 1, 2, 3, 4)$ are real functions of T_1. $\lambda_1 = 0.5\sigma_2$ and $\lambda_2 = 1.5\sigma_2 - \sigma_1$. Substituting Eq (3.19) into Eq (3.18) leads to the following modulation equations [19]:

$$\dot{x}_1 = (\mu_1 - \alpha_1)x_1 + (-\beta_1 + \alpha_2)x_2 + (-k_{22} - k_{82})x_3 + (-k_{21} + k_{81})x_4 + Nf_1^1, \tag{3.20a}$$

$$\dot{x}_2 = (\beta_1 + \alpha_2)x_1 + (\mu_1 + \alpha_1)x_2 + (k_{21} + k_{81})x_3 + (-k_{22} + k_{82})x_4 + Nf_1^2, \tag{3.20b}$$

$$\dot{x}_3 = (-k_{32} - k_{92})x_1 + (-k_{31} + k_{91})x_2 + \mu_2x_3 - \beta_2x_4 + Nf_1^3, \tag{3.20c}$$

$$\dot{x}_4 = (k_{31} + k_{91})x_1 + (-k_{32} + k_{92})x_2 + \beta_2x_3 + \mu_2x_4 + Nf_1^4, \tag{3.20d}$$

where

$$\mu_1 = -\mu C_{1R} - \alpha e_{1R}, \mu_2 = -\mu C_{2R} - \alpha e_{2R}, \beta_1 = 0.5\sigma_2 + \mu C_{1I} + \alpha e_{1I},$$
$$\beta_2 = 1.5\sigma_2 - \sigma_1 + \mu C_{2I} + \alpha e_{2I}, \alpha_1 = K_{1R}, \alpha_2 = K_{1I}.$$

C_{iR}, C_{iI}, e_{iR}, e_{iI}, K_{1R}, K_{1I} are the real and imaginary parts of C_i, e_i, and K_i presented in the Appendix. All the other coefficients and the nonlinear functions Nf_1^i $(i = 1, 2, 3, 4)$ are also summarized in the Appendix.

The Jacobian matrix of Eq (3.20) at the initial equilibrium solutions (E.S.) $x_i = 0$ $(i = 1, 2, 3, 4)$ is as follows:

$$J = \begin{bmatrix} \mu_1 - \alpha_1 & -\beta_1 + \alpha_2 & -k_{22} - k_{82} & -k_{21} + k_{81} \\ \beta_1 + \alpha_2 & \mu_1 + \alpha_1 & k_{21} + k_{81} & -k_{22} + k_{82} \\ -k_{32} - k_{92} & -k_{31} + k_{91} & \mu_2 & -\beta_2 \\ k_{31} + k_{91} & -k_{32} + k_{92} & \beta_2 & \mu_2 \end{bmatrix}, \tag{3.21}$$

from which the characteristic polynomial can be obtained:

$$f(\lambda) = \lambda^4 + b_1\lambda^3 + b_2\lambda^2 + b_3\lambda + b_4, \tag{3.22}$$

where

$$b_1 = -2\mu_1 - 2\mu_2,$$

$$b_2 = h_2(\mu_1, \mu_2, \alpha_1, \alpha_2, \beta_1, \beta_2, k_{21}, k_{22}, k_{31}, k_{32}, k_{81}, k_{82}, k_{91}, k_{92}),$$
$$b_3 = h_3(\mu_1, \mu_2, \alpha_1, \alpha_2, \beta_1, \beta_2, k_{21}, k_{22}, k_{31}, k_{32}, k_{81}, k_{82}, k_{91}, k_{92}),$$
$$b_4 = h_4(\mu_1, \mu_2, \alpha_1, \alpha_2, \beta_1, \beta_2, k_{21}, k_{22}, k_{31}, k_{32}, k_{81}, k_{82}, k_{91}, k_{92}), \tag{3.23}$$

and $h_i(\mu_1, \mu_2, \alpha_1, \alpha_2, \beta_1, \beta_2, k_{21}, k_{22}, k_{31}, k_{32}, k_{81}, k_{82}, k_{91}, k_{92})\,(i = 2, 3, 4)$ are complicated functions provided in the Appendix.

According to the Hurwitz criterion, the stability conditions for $x_i = 0$ $(i = 1, 2, 3, 4)$ can be obtained as follows

$$b_1 > 0,\ b_1 b_2 - b_3 > 0,\ b_4 > 0,\ b_3(b_1 b_2 - b_3) - b_1^2 b_4 > 0. \tag{3.24}$$

If the conditions in Eq (3.24) are violated, the equilibrium solutions may become unstable and then lead to the occurrence of bifurcation. A detailed discussion of codimension-two bifurcations will be carried out in the following section.

4. Stability and bifurcation analysis

In [19], Sahoo et al. analyzed the nonlinear transverse vibration of an axially moving beam using the continuation algorithm. For different control parameters μ, α, ν_1, ν_2, σ_1, and σ_2, numerical results were presented to show the complex nonlinear phenomena of the axially moving beam, and the stability and bifurcation of the equilibrium solution were simultaneously evaluated. However, the stability and bifurcation behaviors of the steady state solutions have not been studied analytically. This study is therefore motivated to investigate the local dynamical behaviors of the axially moving beam both analytically and numerically. The stability regions of the initial equilibrium point and the explicit expressions of the critical bifurcation curves will be discussed in the following analysis.

As we know, damping has a significant influence on dynamical behaviors of the system, so this section mainly focuses on the stability and bifurcation analysis of the two important parameters μ_1 and μ_2, which can be expressed in terms of μ, α, C_{iR}, and e_{iR} $(i = 1, 2)$. It can be divided into three parts based on the type of degenerate equilibrium points, and the eigenvalues of the characteristic polynomial (3.22) include the following three cases:
Case (1) $\lambda_1 = \lambda_2 = 0$, $\lambda_3 = -1$, $\lambda_4 = -3$, which means that $b_1 = 4$, $b_2 = 3$, and $b_3 = b_4 = 0$.
Case (2) $\lambda_1 = 0$, $\lambda_{2,3} = \pm 2i$, $\lambda_4 = -2$, and $b_1 = 2$, $b_2 = 4$, $b_3 = 8$, $b_4 = 0$.
Case (3) $\lambda_{1,2} = \pm\sqrt{3}i$, $\lambda_{3,4} = \pm\sqrt{5}i$, and $b_2 = 8$, $b_1 = b_3 = 0$, $b_4 = 15$.

4.1. The case of a double zero and two negative eigenvalues

For case (1), the system parameters can be determined by Eq (3.23) as
$\mu_1 = -2$, $\mu_2 = 0$, $\alpha_1 = \frac{5}{2}$, $\alpha_2 = 4$, $\beta_1 = \frac{11}{2}$, $\beta_2 = k_{21} = k_{22} = k_{31} = k_{32} = k_{82} = k_{92} = 1$, $k_{81} = 2$,
$k_{91} = 2$, $a_{01} = a_{02} = a_{03} = a_{04} = a_{05} = a_{06} = 1$, $b_{01} = b_{02} = b_{03} = b_{04} = b_{05} = b_{06} = 1$.

Choosing μ_1 and μ_2 as the perturbation parameters, and letting $\mu_1 = -2 + \varsigma_1$, $\mu_2 = \varsigma_2$, Eq (3.22) becomes

$$\bar{f}(\lambda) = \lambda^4 + \bar{b}_1\lambda^3 + \bar{b}_2\lambda^2 + \bar{b}_3\lambda + \bar{b}_4, \tag{4.1}$$

where

$$\bar{b}_1 = -2\varsigma_1 - 2\varsigma_2 + 4,$$

$$\begin{aligned}
\bar{b}_2 &= \varsigma_1^2 + 4\varsigma_1\varsigma_2 + \varsigma_2^2 - 4\varsigma_1 - 8\varsigma_2 + 3,\\
\bar{b}_3 &= -2\varsigma_1^2\varsigma_2 - 2\varsigma_1\varsigma_2^2 + 8\varsigma_1\varsigma_2 + 4\varsigma_2^2 + 8\varsigma_1 - 14\varsigma_2,\\
\bar{b}_4 &= \varsigma_1^2\varsigma_2^2 - 4\varsigma_1\varsigma_2^2 + \varsigma_1^2 - 10\varsigma_1\varsigma_2 + 12\varsigma_2^2.
\end{aligned} \tag{4.2}$$

The stability conditions for $x_i = 0$ $(i = 1, 2, 3, 4)$ are

$$\triangle_1 = \bar{b}_1 > 0,\ \triangle_2 = \bar{b}_1\bar{b}_2 - \bar{b}_3 > 0,\ \triangle_3 = \bar{b}_3\left(\bar{b}_1\bar{b}_2 - \bar{b}_3\right) - \bar{b}_1^2\bar{b}_4 > 0,\ \triangle_4 = \bar{b}_4 > 0, \tag{4.3}$$

i.e.,

$$\begin{aligned}
&-2\varsigma_1 - 2\varsigma_2 + 4 > 0,\\
&-2\varsigma_1^3 - 8\varsigma_1^2\varsigma_2 - 8\varsigma_1\varsigma_2^2 - 2\varsigma_2^3 + 12\varsigma_1^2 + 32\varsigma_1\varsigma_2 + 16\varsigma_2^2 - 30\varsigma_1 - 24\varsigma_2 + 12 > 0,\\
&4\varsigma_1^5\varsigma_2 + 16\varsigma_1^4\varsigma_2^2 + 24\varsigma_1^3\varsigma_2^3 + 16\varsigma_1^2\varsigma_2^4 + 4\varsigma_1\varsigma_2^5 - 40\varsigma_1^4\varsigma_2 - 128\varsigma_1^3\varsigma_2^2 - 144\varsigma_1^2\varsigma_2^3\\
&- 64\varsigma_1\varsigma_2^4 - 8\varsigma_2^5 - 20\varsigma_1^4 + 152\varsigma_1^3\varsigma_2 + 408\varsigma_1^2\varsigma_2^2 + 280\varsigma_1\varsigma_2^3 + 44\varsigma_2^4 + 112\varsigma_1^3 - 320\varsigma_1^2\varsigma_2\\
&- 560\varsigma_1\varsigma_2^2 - 128\varsigma_2^3 - 256\varsigma_1^2 + 484\varsigma_1\varsigma_2 + 192\varsigma_2^2 + 96\varsigma_1 - 168\varsigma_2 > 0,\\
&\varsigma_1^2\varsigma_2^2 - 4\varsigma_1\varsigma_2^2 + \varsigma_1^2 - 10\varsigma_1\varsigma_2 + 12\varsigma_2^2 > 0.
\end{aligned} \tag{4.4}$$

According to Eq (4.4), the following four transition curves are obtained as shown in Figure 2.

$$\begin{aligned}
L_1 &: -2\varsigma_1 - 2\varsigma_2 + 4 = 0,\\
L_2 &: -2\varsigma_1^3 - 8\varsigma_1^2\varsigma_2 - 8\varsigma_1\varsigma_2^2 - 2\varsigma_2^3 + 12\varsigma_1^2 + 32\varsigma_1\varsigma_2 + 16\varsigma_2^2 - 30\varsigma_1 - 24\varsigma_2 + 12 = 0,\\
L_3 &: 4\varsigma_1^5\varsigma_2 + 16\varsigma_1^4\varsigma_2^2 + 24\varsigma_1^3\varsigma_2^3 + 16\varsigma_1^2\varsigma_2^4 + 4\varsigma_1\varsigma_2^5 - 40\varsigma_1^4\varsigma_2 - 128\varsigma_1^3\varsigma_2^2 - 144\varsigma_1^2\varsigma_2^3 - 64\varsigma_1\varsigma_2^4 - 8\varsigma_2^5\\
&\quad - 20\varsigma_1^4 + 152\varsigma_1^3\varsigma_2 + 408\varsigma_1^2\varsigma_2^2 + 280\varsigma_1\varsigma_2^3 + 44\varsigma_2^4 + 112\varsigma_1^3 - 320\varsigma_1^2\varsigma_2 - 560\varsigma_1\varsigma_2^2 - 128\varsigma_2^3\\
&\quad - 256\varsigma_1^2 + 484\varsigma_1\varsigma_2 + 192\varsigma_2^2 + 96\varsigma_1 - 168\varsigma_2 = 0,\\
L_4 &: \varsigma_1^2\varsigma_2^2 - 4\varsigma_1\varsigma_2^2 + \varsigma_1^2 - 10\varsigma_1\varsigma_2 + 12\varsigma_2^2 = 0,
\end{aligned} \tag{4.5}$$

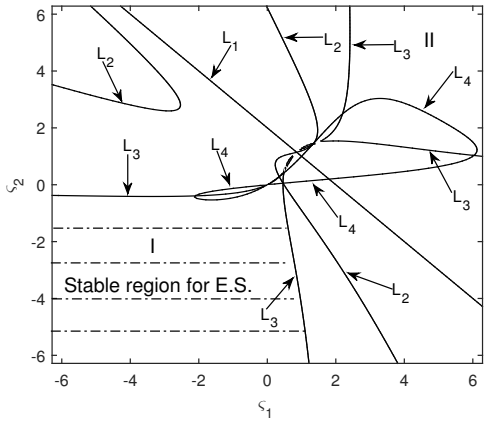

Figure 2. Transition curves for $\lambda_1 = \lambda_2 = 0$, $\lambda_3 = -1$, $\lambda_4 = -3$.

It is obvious that the E.S. is stable when the parameters ς_1 and ς_2 are located in region I shown in Figure 2. Possible bifurcations may occur from the stable solution $x_i = 0$ $(i = 1, 2, 3, 4)$ when the parameters ς_1 and ς_2 are chosen from region II.

Employing the fourth-order Runge-Kutta method, numerical results have been obtained on the basis of the Eq (3.20). Choosing the parameter values $(\varsigma_1, \varsigma_2) = (0.1, -0.5)$ from region I, a numerical solution starting from an initial point $(x_1, x_2, x_3, x_4) = (0.03, -0.02, -0.05, 0.02)$ asymptotically converges to the region of the origin, shown in Figure 3, and it is proved that the E.S. is stable. See Figure 3 for the phase trajectories on the $x_1 - x_2$ and $x_3 - x_4$ subspaces. If the values of ς_1 and ς_2 are determined from the region II, the E.S. becomes unstable.

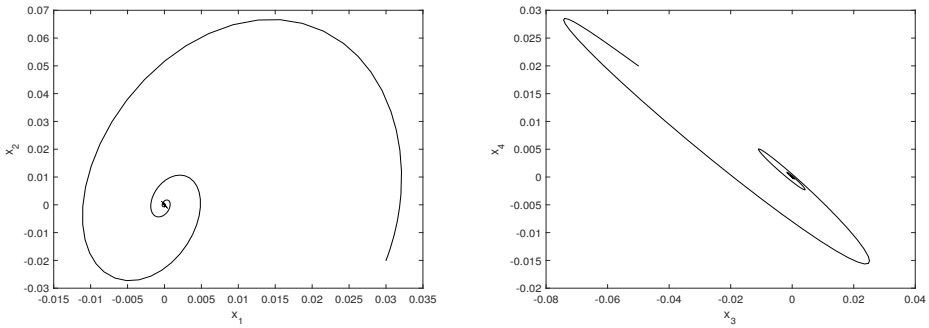

(a) (b)

Figure 3. The trajectory starting from $(x_1, x_2, x_3, x_4) = (0.03, -0.02, -0.05, 0.02)$ converges to the E.S. for $(\varsigma_1, \varsigma_2) = (0.1, -0.5)$. (a) The phase portrait on plane (x_1, x_2); (b) the phase portrait on plane (x_3, x_4).

4.2. The case of a simple zero and a pair of pure imaginary eigenvalues

In case (2), the parameter values are selected as

$\mu_1 = -1, \mu_2 = 0, \alpha_1 = 0, \alpha_2 = 1, \beta_1 = 0, \beta_2 = -2, k_{21} = \frac{1}{2}, k_{81} = \frac{3}{2}, k_{22} = k_{31} = k_{32} = k_{82} = k_{91} = k_{92} = 0, a_{01} = a_{02} = a_{03} = a_{04} = a_{05} = a_{06} = 1, b_{01} = b_{02} = b_{03} = b_{04} = b_{05} = b_{06} = 1.$

Choosing μ_1 and μ_2 as the perturbation parameters, letting $\mu_1 = -1 + \varsigma_1$, $\mu_2 = \varsigma_2$, and applying the state variable transformation

$$\begin{bmatrix} x_1 \\ x_2 \\ x_3 \\ x_4 \end{bmatrix} = \begin{bmatrix} 1 & \frac{1}{2} & -\frac{3}{4} & -1 \\ 1 & 1 & -\frac{19}{4} & 1 \\ 0 & 5 & -1 & 0 \\ 0 & 1 & 5 & 0 \end{bmatrix} \begin{bmatrix} z_1 \\ z_2 \\ z_3 \\ z_4 \end{bmatrix} \tag{4.6}$$

onto Eq (3.20) yield

$$\dot{z}_1 = \varsigma_1 z_1 + \left(\frac{3}{4}\varsigma_1 - \frac{3}{4}\varsigma_2\right) z_2 + \left(-\frac{11}{4}\varsigma_1 + \frac{11}{4}\varsigma_2\right) z_3 + N f_2^1, \tag{4.7a}$$

$$\dot{z}_2 = 2z_3 + \varsigma_2 z_2 + N f_2^2, \tag{4.7b}$$

$$\dot{z}_3 = -2z_2 + \varsigma_2 z_3 + N f_2^3, \tag{4.7c}$$

$$\dot{z}_4 = -2z_4 + \left(\frac{1}{4}\varsigma_1 - \frac{1}{4}\varsigma_2\right) z_2 + (-2\varsigma_1 + 2\varsigma_2) z_3 + \varsigma_1 z_4 + N f_2^4, \tag{4.7d}$$

where the nonlinear functions $Nf_2^i\,(i = 1, 2, 3, 4)$ are listed in the Appendix. Evaluating on the solution $z_i = 0$ at the critical point $\varsigma_{1c} = \varsigma_{2c} = 0$, the Jacobian matrix of Eq (4.7) can be achieved as

$$J_{(z_i=0)} = \begin{bmatrix} 0 & 0 & 0 & 0 \\ 0 & 0 & 2 & 0 \\ 0 & -2 & 0 & 0 \\ 0 & 0 & 0 & -2 \end{bmatrix}. \tag{4.8}$$

Note that the local dynamical behaviors of the system in the vicinity of the critical point are related to the critical variables z_1, z_2, and z_3. According to Eq (4.7), the research in [20] are applied to determine the normal form of system (4.7) as follows:

$$\begin{aligned} \dot{y} &= y\left(\varsigma_1 - 4y^2 - \frac{1365}{16}r^2\right), \\ \dot{r} &= r\left(\varsigma_2 + \frac{7}{4}y^2 - \frac{9347}{256}r^2\right), \end{aligned} \tag{4.9}$$

and

$$\dot{\theta} = 2 - \frac{11}{4}y^2 - \frac{12701}{256}r^2. \tag{4.10}$$

Letting $\dot{y} = \dot{r} = 0$ in Eq (4.9) yields the following steady state solutions.

The initial equilibrium solution (E.S.):

$$y = r = 0. \tag{4.11}$$

The static bifurcation solution (S.B.):

$$\begin{cases} y^2 = \dfrac{1}{4}\varsigma_1, \\ r = 0. \end{cases} \tag{4.12}$$

The Hopf bifurcation solution (H.B. with frequency ω_1):

$$\begin{cases} y = 0, \\ r^2 = \dfrac{256}{9347}\varsigma_2. \end{cases} \tag{4.13}$$

The secondary Hopf bifurcation or the secondary static bifurcation solution (2nd H.B. or 2nd S.B. with frequency ω_2):

$$\begin{cases} y^2 = \dfrac{719}{5816}\varsigma_1 - \dfrac{210}{727}\varsigma_2, \\ r^2 = \dfrac{56}{9451}\varsigma_1 + \dfrac{128}{9451}\varsigma_2. \end{cases} \tag{4.14}$$

Note that the characters of Eqs (4.11)–(4.14) can be verified based on the Jacobian matrix of (4.9), given by

$$J = \begin{bmatrix} \varsigma_1 - 12y^2 - \dfrac{1365}{16}r^2 & -\dfrac{1365}{8}yr \\ \dfrac{7}{2}yr & \varsigma_2 - \dfrac{28041}{256}r^2 + \dfrac{7}{4}y^2 \end{bmatrix}. \tag{4.15}$$

Evaluating (4.15) on (4.11) reveals that the stability of the E.S. can be rigorously established under the following conditions:

$$\varsigma_1 < 0 \quad and \quad \varsigma_2 < 0. \tag{4.16}$$

The region obtained by Eq (4.16) is exhibited in Figure 4, which illustrates the stability boundaries for the E.S., which are

$$L_5 : \ \varsigma_1 = 0 \quad (\varsigma_2 < 0), \tag{4.17}$$

where the S.B. solution given by Eq (4.12) bifurcates from the E.S. (4.11). The other critical line is

$$L_6 : \ \varsigma_2 = 0 \quad (\varsigma_1 < 0), \tag{4.18}$$

along which the H.B. solution (4.13) naturally emerges.

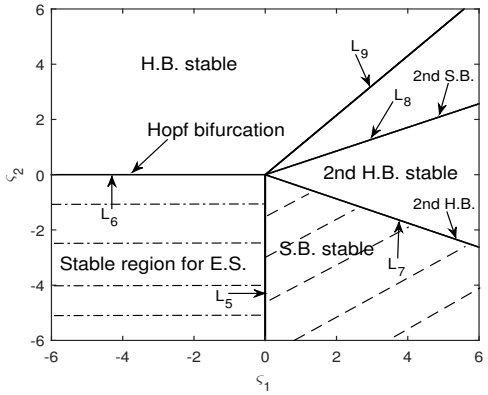

Figure 4. Transition curves for $\lambda_1 = 0$, $\lambda_{2,3} = \pm 2i$, $\lambda_4 = -2$.

To determine the stability conditions for (4.12), the Jacobian matrix (4.15) on the S.B. solution (4.12) is evaluated as

$$J_{\text{S.B.}} = \begin{bmatrix} -2\varsigma_1 & 0 \\ 0 & \varsigma_2 + \dfrac{7}{16}\varsigma_1 \end{bmatrix}, \tag{4.19}$$

which means that the S.B. solution maintains its stability if

$$\varsigma_1 > 0 \quad and \quad 16\varsigma_2 + 7\varsigma_1 < 0. \tag{4.20}$$

The stability boundaries decided by conditions (4.20) comprise both the critical line L_5 and an additional critical line

$$L_7 : \ 16\varsigma_2 + 7\varsigma_1 = 0 \quad (\varsigma_1 > 0). \tag{4.21}$$

It is confirmed that the stability criterion for the S.B. solution (4.12) is strictly satisfied within the domain enclosed between L_5 and L_7 (see Figure 4).

Similarly, the Jacobian matrix (4.15) on Eq (4.13) is calculated to yield

$$J_{\text{H.B.}} = \begin{bmatrix} \varsigma_1 - \dfrac{1680}{719}\varsigma_2 & 0 \\ 0 & -2\varsigma_2 \end{bmatrix}, \tag{4.22}$$

which implies the stability of the H.B. solution when the following conditions hold:

$$719\varsigma_1 - 1680\varsigma_2 < 0 \quad and \quad \varsigma_2 > 0, \tag{4.23}$$

and the frequency of (4.13) is expressed as

$$\omega_1 = 2 - \frac{977}{719}\varsigma_2. \tag{4.24}$$

Consequently, the stability region of the H.B. solution is bounded between two critical boundaries: the critical line L_6 and an additional critical line characterized by

$$L_8 : \ 719\varsigma_1 - 1680\varsigma_2 = 0 \quad (\varsigma_2 > 0). \tag{4.25}$$

It is noted that the critical boundary L_7 is intersected with the change of the parameter values, and the S.B. solution given by Eq (4.12) loses stability and undergoes a bifurcation, giving rise to a family of limit cycles known as the 2nd H.B. solution (4.14). It is further demonstrated that the H.B. solution presented in (4.13) becomes unstable when crossing the critical boundary L_8, from which another family of limit cycles identified as the 2nd S.B. solution (4.14) emerges. The frequency of the 2nd H.B./2nd S.B. solution is determined as

$$\omega_2 = 2 - \frac{3687}{5816}\varsigma_1 + \frac{89}{727}\varsigma_2. \tag{4.26}$$

To analyze the stability of (4.14), the Jacobian matrix (4.15) on Eq (4.14) is computed to derive

$$J_{2\text{nd H.B.}} = \begin{bmatrix} -8y^2 & -\frac{1365}{8}yr \\ \frac{7}{2}yr & -\frac{9347}{128}r^2 \end{bmatrix}. \tag{4.27}$$

The stability conditions for (4.14) are determined by analyzing the trace and determinant of (4.27) given as follows:

$$\text{Tr} = -8y^2 - \frac{9347}{128}r^2 = -\frac{16537}{11632}\varsigma_1 + \frac{961}{727}\varsigma_2 < 0, \tag{4.28}$$

$$\text{Det} = \frac{9451}{8}y^2r^2 = \frac{1}{5816}(719\varsigma_1 - 1680\varsigma_2)(16\varsigma_2 + 7\varsigma_1) > 0. \tag{4.29}$$

Obviously, the fulfillment of condition (4.29) becomes inherently guaranteed whenever the 2nd H.B. solution exists. Setting the determinant equal to zero results in L_7 and L_8 that demarcate the parameter region for the existence of the 2nd H.B. solutions. Letting the trace equal zero, an additional critical line is established as

$$L_9 : \ -16537\varsigma_1 + 15376\varsigma_2 = 0. \tag{4.30}$$

Theoretical analysis suggests the potential emergence of a two-dimensional (2-D) torus through secondary bifurcation. However, our investigation reveals that the critical line L_9 (with slope 1.076) lies strictly above L_8 (slope 0.428). Consequently, the 2nd H.B. solutions cannot undergo a

bifurcation into a two-dimensional torus. Therefore, the existence of a 2nd H.B. solution ensures its stability. The corresponding critical bifurcation lines are depicted in Figure 4.

Similar to the case in Subsection 4.1, parameter values are selected from distinct regions in Figure 4 to verify the analytical results derived in this section. Choosing the parameter values $(\varsigma_1, \varsigma_2) = (-0.1, -0.1)$ within the stable region of the E.S., the trajectory originating from $(x_1, x_2, x_3, x_4) = (0.01, -0.02, 0.03, 0.04)$ asymptotically converges to the origin, as demonstrated in Figure 5. When the parameter values are set to $(\varsigma_1, \varsigma_2) = (0.1, -0.1)$ within the stable region of the S.B. solution, numerical simulation demonstrates that the trajectory originating from the initial condition $(x_1, x_2, x_3, x_4) = (-0.2, 0.02, -0.1, 0.01)$ asymptotically converges to the S.B. solution shown in Figure 6. When selecting $(\varsigma_1, \varsigma_2) = (-0.1, 0.1)$, numerical simulations reveal a stable limit cycle as demonstrated in Figure 7. The periodic trajectory associated with the H.B. solution originates from the initial condition $(x_1, x_2, x_3, x_4) = (-0.02, 0.03, 0.02, -0.01)$. Furthermore, when employing parameter values $(\varsigma_1, \varsigma_2) = (0.3, 0.1)$ within the stable region for the 2nd H.B. solution, the system generates another stable limit cycle from initial coordinates $(x_1, x_2, x_3, x_4) = (0.01, 0.04, -0.02, 0.03)$, as illustrated in Figure 8. Notably, all numerical simulations show qualitative agreement with analytical predictions.

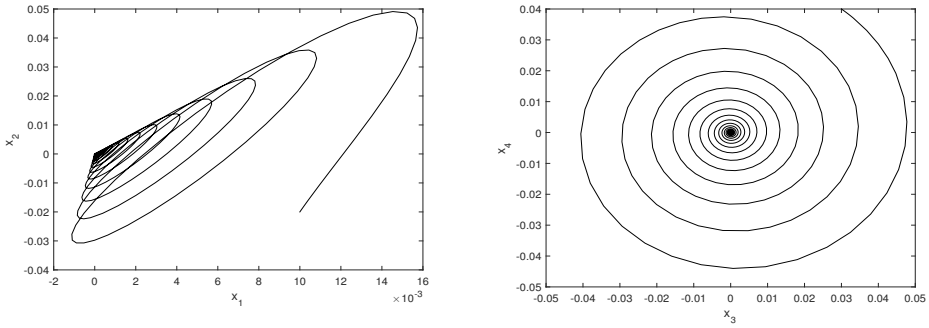

(a) (b)

Figure 5. The trajectory starting from $(x_1, x_2, x_3, x_4) = (0.01, -0.02, 0.03, 0.04)$ converges to the E.S. for $(\varsigma_1, \varsigma_2) = (-0.1, -0.1)$.

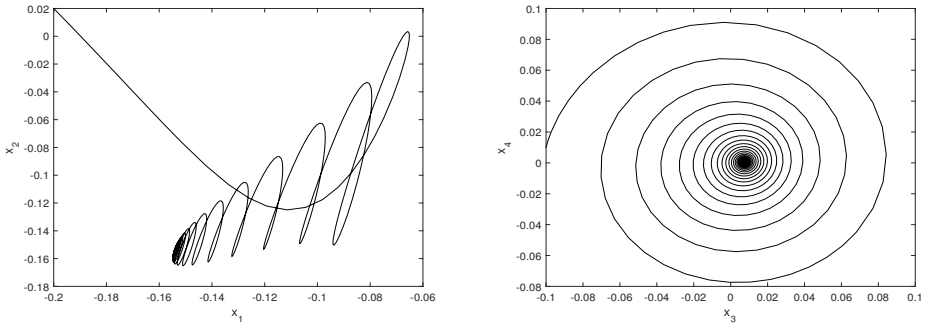

(a) (b)

Figure 6. The trajectory starting from $(x_1, x_2, x_3, x_4) = (-0.2, 0.02, -0.1, 0.01)$ converges to the S.B. for $(\varsigma_1, \varsigma_2) = (0.1, -0.1)$.

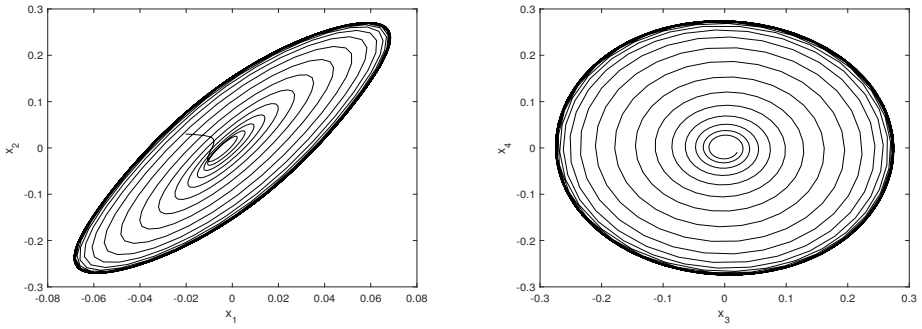

(a) (b)

Figure 7. The trajectory starting from $(x_1, x_2, x_3, x_4) = (-0.02, 0.03, 0.02, -0.01)$ converges to the H.B. for $(\varsigma_1, \varsigma_2) = (-0.1, 0.1)$.

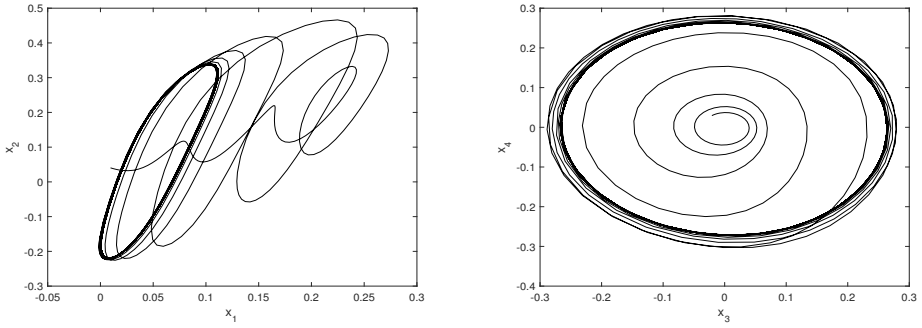

(a) (b)

Figure 8. The trajectory starting from $(x_1, x_2, x_3, x_4) = (0.01, 0.04, -0.02, 0.03)$ converges to the 2nd H.B. for $(\varsigma_1, \varsigma_2) = (0.3, 0.1)$.

4.3. The case of two pairs of pure imaginary eigenvalues

Similarly, for the third case described above, the parameter values can be established as

$\mu_1 = 1, \mu_2 = -1, \alpha_1 = \alpha_2 = 0, \beta_1 = \beta_2 = 0, k_{21} = 2, k_{31} = 3, k_{81} = k_{91} = 1, k_{22} = k_{32} = k_{82} = k_{92} = 0$, $a_{01} = a_{02} = a_{03} = a_{04} = a_{05} = a_{06} = 1$, $b_{01} = b_{02} = b_{03} = b_{04} = b_{05} = b_{06} = 1$.

Choosing μ_1 and μ_2 as the perturbation parameters, applying the parameter transformation $\mu_1 = 1 + \varsigma_1, \mu_2 = -1 + \varsigma_2$, and taking into account the state variable transformation

$$\begin{bmatrix} x_1 \\ x_2 \\ x_3 \\ x_4 \end{bmatrix} = \begin{bmatrix} -\frac{\sqrt{3}}{2} & -\frac{1}{2} & 0 & 0 \\ 0 & 0 & \sqrt{5} & 2 \\ 0 & 0 & -\sqrt{5} & 1 \\ -\sqrt{3} & 1 & 0 & 0 \end{bmatrix} \begin{bmatrix} z_1 \\ z_2 \\ z_3 \\ z_4 \end{bmatrix}. \tag{4.31}$$

Equation (3.20) becomes

$$\dot{z}_1 = \sqrt{3} z_2 + \frac{1}{2}(\varsigma_1 + \varsigma_2) z_1 + \left(\frac{\sqrt{3}}{6} \varsigma_1 - \frac{\sqrt{3}}{6} \varsigma_2 \right) z_2 + N f_3^1, \tag{4.32a}$$

$$\dot{z}_2 = -\sqrt{3}z_1 + \left(\frac{\sqrt{3}}{2}\varsigma_1 - \frac{\sqrt{3}}{2}\varsigma_2\right)z_1 + \frac{1}{2}(\varsigma_1 + \varsigma_2)z_2 + Nf_3^2, \tag{4.32b}$$

$$\dot{z}_3 = \sqrt{5}z_4 + \left(\frac{1}{3}\varsigma_1 + \frac{2}{3}\varsigma_2\right)z_3 + \left(\frac{2\sqrt{5}}{15}\varsigma_1 - \frac{2\sqrt{5}}{15}\varsigma_2\right)z_4 + Nf_3^3, \tag{4.32c}$$

$$\dot{z}_4 = -\sqrt{5}z_3 + \left(\frac{\sqrt{5}}{3}\varsigma_1 - \frac{\sqrt{5}}{3}\varsigma_2\right)z_3 + \left(\frac{2}{3}\varsigma_1 + \frac{1}{3}\varsigma_2\right)z_4 + Nf_3^4, \tag{4.32d}$$

where the nonlinear functions $Nf_3^i (i = 1, 2, 3, 4)$ are presented in the Appendix. At the critical point $\varsigma_{1c} = \varsigma_{2c} = 0$, the Jacobian matrix of Eq (4.32) evaluated with respect to the initial equilibrium solution $z_i = 0$ takes the following canonical form:

$$J_{(z_i=0)} = \begin{bmatrix} 0 & \sqrt{3} & 0 & 0 \\ -\sqrt{3} & 0 & 0 & 0 \\ 0 & 0 & 0 & \sqrt{5} \\ 0 & 0 & -\sqrt{5} & 0 \end{bmatrix}. \tag{4.33}$$

Applying the normal form theory, performing a near-identity nonlinear transformation $z_i = y_i + g_i(y_j)$, and then implementing a transformation $y_1 = r_1\cos\theta_1$, $y_2 = r_1\sin\theta_1$, $y_3 = r_2\cos\theta_2$, $y_4 = r_2\sin\theta_2$, the normal form of Eq (4.32) can be derived as follows [20]:

$$\begin{aligned} \dot{r}_1 &= r_1\left(\frac{1}{2}\varsigma_1 + \frac{1}{2}\varsigma_2 - \frac{11}{4}r_1^2 - 9r_2^2\right), \\ \dot{r}_2 &= r_2\left(\frac{1}{2}\varsigma_1 + \frac{1}{2}\varsigma_2 - 2r_1^2 - \frac{27}{4}r_2^2\right), \end{aligned} \tag{4.34}$$

and

$$\begin{aligned} \dot{\theta}_1 &= \sqrt{3} - \frac{\sqrt{3}}{6}\varsigma_1 + \frac{\sqrt{3}}{6}\varsigma_2 + \frac{3\sqrt{3}}{8}r_1^2 - \frac{19\sqrt{3}}{4}r_2^2, \\ \dot{\theta}_2 &= \sqrt{5} - \frac{\sqrt{5}}{10}\varsigma_1 + \frac{\sqrt{5}}{10}\varsigma_2 + \frac{9\sqrt{5}}{20}r_1^2 - \frac{21\sqrt{5}}{8}r_2^2. \end{aligned} \tag{4.35}$$

According to Eq (4.34), the steady state solutions can be acquired by setting $\dot{r}_1 = \dot{r}_2 = 0$.
The initial equilibrium solution (E.S.):

$$r_1 = r_2 = 0 \quad (i.e., z_i = 0). \tag{4.36}$$

The incipient Hopf bifurcation solution (H.B.(I) with frequency ω_1):

$$r_1^2 = \frac{2}{11}(\varsigma_1 + \varsigma_2), \quad r_2 = 0, \tag{4.37}$$

$$\omega_1 = \sqrt{3} - \frac{13\sqrt{3}}{132}\varsigma_1 + \frac{31\sqrt{3}}{132}\varsigma 2. \tag{4.38}$$

The secondary Hopf bifurcation solution (H.B.(II) with frequency ω_2):

$$r_1 = 0, \quad r_2^2 = \frac{2}{27}(\varsigma_1 + \varsigma_2), \tag{4.39}$$

$$\omega_2 = \sqrt{5} - \frac{53\sqrt{5}}{180}\varsigma_1 - \frac{17\sqrt{5}}{180}\varsigma 2. \tag{4.40}$$

Quasi-periodic solution (2-D tori):

$$r_1^2 = -2(\varsigma_1 + \varsigma_2), \quad r_2^2 = \frac{2}{3}(\varsigma_1 + \varsigma_2). \tag{4.41}$$

The Jacobian matrix of Eq (4.34) can be expressed in the following form:

$$J = \begin{bmatrix} \frac{1}{2}\varsigma_1 + \frac{1}{2}\varsigma_2 - \frac{33}{4}r_1^2 - 9r_2^2 & -18r_1r_2 \\ -4r_1r_2 & \frac{1}{2}\varsigma_1 + \frac{1}{2}\varsigma_2 - 2r_1^2 - \frac{81}{4}r_2^2 \end{bmatrix}, \tag{4.42}$$

which can be applied to assess the stability of the four steady state solutions mentioned above. Evaluating (4.42) on (4.36) yields the stability region of E.S. as

$$\varsigma_1 + \varsigma_2 < 0, \tag{4.43}$$

which gives the critical line defined by

$$L_{10} : \ \varsigma_1 + \varsigma_2 = 0, \tag{4.44}$$

from which a family of limit cycles emerges from the E.S. through a Hopf bifurcation, with the H.B.(II) solution being expressed as Eq (4.39).

Evaluating the Jacobian matrix (4.42) on (4.37) leads to the stability conditions

$$\varsigma_1 + \varsigma_2 < 0 \quad \textit{and} \quad \varsigma_1 + \varsigma_2 > 0, \tag{4.45}$$

which are contradictive, which reveals that the H.B.(I) exhibits instability.

Similarly, evaluating (4.42) on (4.39) yields the stability condition as

$$\varsigma_1 + \varsigma_2 > 0. \tag{4.46}$$

The next task is to find the stability conditions for 2-D tori given by Eq (4.41), while the expression of the quasi-periodic solution shows that no quasi-periodic solutions exist unless $r_1 = r_2 = 0$.

From the previous analysis, it can be concluded that when L_{10} is intersected with the change of the parameter values, the E.S. (4.36) loses stability and undergoes a Hopf bifurcation, resulting in the emergence of stable limit cycles (H.B.(II) solution). The critical bifurcation line is illustrated in Figure 9.

In this case, the parameter values are selected from distinct regions in Figure 9 to find the numerical solutions. Choosing $(\varsigma_1, \varsigma_2) = (-0.8, 0.1)$ within the stable region of the E.S., the trajectory originating from $(x_1, x_2, x_3, x_4) = (-0.03, -0.02, 0.01, 0.02)$ asymptotically converges to the origin, as can be seen in Figure 10. Choosing the parameter values as $(\varsigma_1, \varsigma_2) = (0.2, -0.1)$ within the stable region of the H.B.(II) solution, the system's trajectory evolves into a stable limit cycle from initial coordinates $(x_1, x_2, x_3, x_4) = (0.03, -0.01, -0.02, 0.04)$, depicted in Figure 11. It is observed that all numerical solutions exhibit excellent agreement with analytical results.

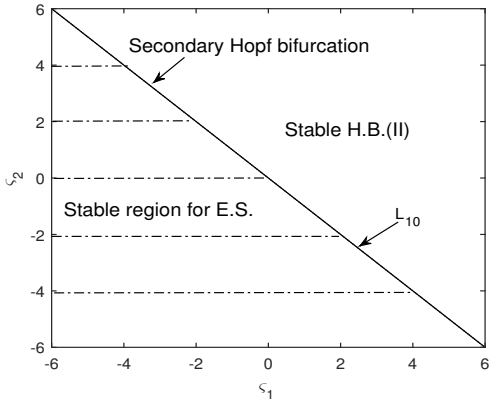

Figure 9. Transition curves for $\lambda_{1,2} = \pm\sqrt{3}i$, $\lambda_{3,4} = \pm\sqrt{5}i$.

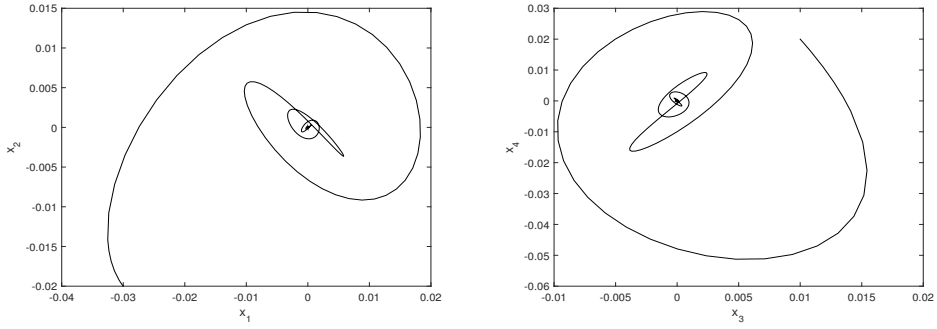

(a) (b)

Figure 10. The trajectory starting from $(x_1, x_2, x_3, x_4) = (-0.03, -0.02, 0.01, 0.02)$ converges to the E.S. for $(\varsigma_1, \varsigma_2) = (-0.8, 0.1)$.

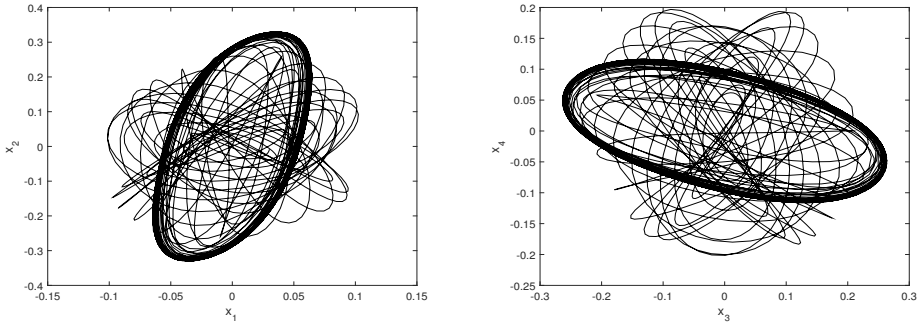

(a) (b)

Figure 11. The trajectory starting from $(x_1, x_2, x_3, x_4) = (0.03, -0.01, -0.02, 0.04)$ converges to the H.B.(II) solution for $(\varsigma_1, \varsigma_2) = (0.2, -0.1)$.

5. Conclusions

In this paper, stability and bifurcation behaviors of an axially moving beam subjected to two frequency parametric excitations are studied. Simultaneous principal parametric resonance as well as

combination parametric resonance with 3:1 internal resonance is considered. Three types of degenerated equilibrium points are discussed in detail. Based on the aforementioned research, the following conclusions are obtained:

(1) The steady state solutions are analytically derived and their stability conditions are determined as explicit expressions of the parameters ς_1 and ς_2, which are obtained by using the parameter transformations in three cases: (1) $\mu_1 = -2 + \varsigma_1, \mu_2 = \varsigma_2$; (2) $\mu_1 = -1 + \varsigma_1$, $\mu_2 = \varsigma_2$; (3) $\mu_1 = 1 + \varsigma_1$, $\mu_2 = -1 + \varsigma_2$, where $\mu_1 = -\mu C_{1R} - \alpha e_{1R}$, $\mu_2 = -\mu C_{2R} - \alpha e_{2R}$. μ is a coefficient that denotes the nondimensional viscous (external) damping. α is another coefficient of nondimensional material (internal) damping. C_{iR} and e_{iR} $(i = 1, 2)$ are the real parts of the nonlinear interaction coefficients C_i and e_i. As mentioned above, the parameters ς_1 and ς_2 are related to μ, α, C_{iR}, and e_{iR} $(i = 1, 2)$, which indicates that the stability conditions and the dynamical behaviors are affected by the viscous (external) damping μ, the material (internal) damping α, and the nonlinear interaction coefficients C_{iR} and e_{iR} $(i = 1, 2)$ of the system. It is further demonstrated that complex dynamical behaviors of the traveling viscoelastic beams can be controlled by modifying the parameters μ and α. Therefore, the theoretical studies obtained here can help us to optimize the design of the structural parameters of accelerating beams. In addition, transition curves giving rise to static bifurcation, Hopf bifurcation, and 2-D torus bifurcation are discussed applying normal form theory, stability, and bifurcation theory.

(2) In order to confirm the analytical predictions, system (3.20) is chosen to conduct numerical simulations. The fourth-order Runge-Kutta algorithm through the software MATLAB is employed to indicate stability of the steady state solutions. It is observed that all the numerical simulations agree with the theoretical predictions. In the design of vehicles, such as spacecrafts, automobiles, and aerial cable tramways, the structural components may demonstrate a significant nonlinear behavior that requires careful consideration and precise control. The results of this study could provide critical insights for mechanical engineers specializing in the nonlinear vibration analysis of axially moving beams.

Author contributions

Fengxian An: Methodology, Software, Writing-original draft; Liangqiang Zhou: Methodology, Writing-reviewing and editing. All authors have read and approved the final version of the manuscript for publication.

Use of Generative-AI tools declaration

The authors declare they have not used Artificial Intelligence (AI) tools in the creation of this article.

Acknowledgments

This research was supported by the Open Foundation of Key Laboratory of Mathematical Modelling and High Performance Computing of Air Vehicles (NUAA) (No. 202301) and the National Natural Science Foundation of China (No. 11772148).

Conflict of interest

The authors declare no conflict of interest in this paper.

References

1. P. Lad, V. Kartik, Bifurcations and chaos in the dynamics of an axially moving string impacting a distributed unilateral foundation, *J. Sound Vib.*, **589** (2024), 118545. http://dx.doi.org/10.1016/j.jsv.2024.118545
2. Y. D. Hu, Y. X. Tian, Primary parametric resonance, stability analysis and bifurcation characteristics of an axially moving ferromagnetic rectangular thin plate under the action of air-gap field, *Nonlinear Dyn.*, **112** (2024), 8889–8920. http://dx.doi.org/10.1007/s11071-024-09457-3
3. L. Chen, Y. Q. Tang, Bifurcation and chaos of axially moving beams under time-varying tension, *Chin. J. Theor. Appl. Mech.*, **51** (2019), 1180–1188. http://dx.doi.org/10.6052/0459-1879-19-068
4. H. R. Öz, M. Pakdemirli, Two-to-one internal resonances in a shallow curved beam resting on an elastic foundation, *Acta Mech.*, **185** (2006), 245–260. http://dx.doi.org/10.1007/s00707-006-0352-5
5. O. O. Ozgumus, M. O. Kaya, Flapwise bending vibration analysis of double tapered rotating Euler-Bernoulli beam by using the differential transform method, *Meccanica*, **41** (2006), 661–670. http://dx.doi.org/10.1007/s11012-006-9012-z
6. O. O. Ozgumus, M. O. Kaya, Vibration analysis of a rotating tapered Timoshenko beam using DTM, *Meccanica*, **45** (2010), 33–42. http://dx.doi.org/10.1007/s11012-009-9221-3
7. T. A. Apalara1, A. O. Ige, C. D. Enyi, M. E. Omaba, Uniform stability result of laminated beams with thermoelasticity of type III, *AIMS Math.*, **8** (2022), 1090–1101. http://dx.doi.org/10.3934/math.2023054
8. K. Y. Sze, S. H. Chen, J. L. Huang, The incremental harmonic balance method for non-linear vibration of axially moving beams, *J. Sound Vib.*, **281** (2005), 611–626. http://dx.doi.org/10.1016/j.jsv.2004.01.012
9. X. D. Yang, L. Q. Chen, Bifurcation and chaos of an axially accelerating viscoelastic beam, *Chaos Solitons Fract.*, **23** (2005), 249–258. http://dx.doi.org/10.1016/j.chaos.2004.04.008
10. C. An, J. Su, Dynamic response of clamped axially moving beams: Integral transform solution, *Appl. Math. Comput.*, **218** (2011), 249–259. http://dx.doi.org/10.1016/j.amc.2011.05.035
11. S. Rajasekaran, Buckling and vibration of axially functionally graded nonuniform beams using differential transformation based dynamic stiffness approach, *Meccanica*, **48** (2013), 1053–1070. http://dx.doi.org/10.1007/s11012-012-9651-1
12. W. Zhang, D. M. Wang, M. H. Yao, Using Fourier differential quadrature method to analyze transverse nonlinear vibrations of an axially accelerating viscoelastic beam, *Nonlinear Dyn.*, **78** (2014), 839–856. http://dx.doi.org/10.1007/s11071-014-1481-3
13. Q. Y. Yan, H. Ding, L. Q. Chen, Periodic responses and chaotic behaviors of an axially accelerating viscoelastic Timoshenko beam, *Nonlinear Dyn.*, **78** (2014), 1577–1591. http://dx.doi.org/10.1007/s11071-014-1535-6

14. Y. Q. Tang, D. B. Zhang, J. M. Gao, Parametric and internal resonance of axially accelerating viscoelastic beams with the recognition of longitudinally varying tensions, *Nonlinear Dyn.*, **83** (2016), 401–418. http://dx.doi.org/10.1007/s11071-015-2336-2

15. A. Moslemi, S. E. Khadem, M. Khazaee, A. Davarpanah, Nonlinear vibration and dynamic stability analysis of an axially moving beam with a nonlinear energy sink, *Nonlinear Dyn.*, **104** (2021), 1955–1972. http://dx.doi.org/10.1007/s11071-021-06389-0

16. Y. Hao, H. L. Dai, N. Qiao, L. Wang, Dynamics and stability analysis of an axially moving beam in axial flow, *J. Mech. Mater. Struct.*, **15** (2020), 37–60. http://dx.doi.org/10.2140/jomms.2020.15.37

17. L. Chen, Y. Q. Tang, S. Liu, Y. Zhou, X. G. Liu, Nonlinear phenomena in axially moving beams with speed-dependent tension and tension-dependent speed, *Int. J. Bifurcat. Chaos*, **31** (2021), 2150037. http://dx.doi.org/10.1142/S0218127421500371

18. Q. L. Wu, G. Y. Qi, Homoclinic bifurcations and chaotic dynamics of non-planar waves in axially moving beam subjected to thermal load, *Appl. Math. Model.*, **83** (2020), 674–682. http://dx.doi.org/10.1016/j.apm.2020.03.013

19. B. Sahoo, L. N. Panda, G. Pohit, Combination, principal parametric and internal resonances of an accelerating beam under two frequency parametric excitation, *Int. J. Non-Linear Mech.*, **78** (2016), 35–44. http://dx.doi.org/10.1016/j.ijnonlinmec.2015.09.017

20. P. Yu, Analysis on double Hopf bifurcation using computer algebra with the aid of multiple scales, *Nonlinear Dyn.*, **27** (2002), 19–53. http://dx.doi.org/10.1023/A:1017993026651

Appendix

$$C_1 = \frac{-\mathrm{i}\omega_1 \int_0^1 \phi_1\bar{\phi}_1 \mathrm{d}x}{-\{\mathrm{i}\omega_1 \int_0^1 \phi_1\bar{\phi}_1 \mathrm{d}x + v_0 \int_0^1 \phi_1'\bar{\phi}_1 \mathrm{d}x\}}, \quad C_2 = \frac{-\mathrm{i}\omega_2 \int_0^1 \phi_2\bar{\phi}_2 \mathrm{d}x}{-\{\mathrm{i}\omega_2 \int_0^1 \phi_2\bar{\phi}_2 \mathrm{d}x + v_0 \int_0^1 \phi_2'\bar{\phi}_2 \mathrm{d}x\}},$$

$$e_1 = \frac{-\mathrm{i}\omega_1 \int_0^1 \phi_1''''\bar{\phi}_1 \mathrm{d}x}{-\{\mathrm{i}\omega_1 \int_0^1 \phi_1\bar{\phi}_1 \mathrm{d}x + v_0 \int_0^1 \phi_1'\bar{\phi}_1 \mathrm{d}x\}}, \quad e_2 = \frac{-\mathrm{i}\omega_2 \int_0^1 \phi_2''''\bar{\phi}_2 \mathrm{d}x}{-\{\mathrm{i}\omega_2 \int_0^1 \phi_2\bar{\phi}_2 \mathrm{d}x + v_0 \int_0^1 \phi_2'\bar{\phi}_2 \mathrm{d}x\}},$$

$$K_1 = \frac{\frac{1}{2}\{v_1\omega_1 \int_0^1 \bar{\phi}_1'\bar{\phi}_1 \mathrm{d}x - \frac{v_1\Omega_1}{2} \int_0^1 \bar{\phi}_1'\bar{\phi}_1 \mathrm{d}x + \mathrm{i}v_0v_1 \int_0^1 \bar{\phi}_1''\bar{\phi}_1 \mathrm{d}x\}}{-\{\mathrm{i}\omega_1 \int_0^1 \phi_1\bar{\phi}_1 \mathrm{d}x + v_0 \int_0^1 \phi_1'\bar{\phi}_1 \mathrm{d}x\}},$$

$$K_2 = \frac{\frac{1}{2}\{v_1\omega_2 \int_0^1 \phi_2'\bar{\phi}_1 \mathrm{d}x - \frac{v_1\Omega_1}{2} \int_0^1 \phi_2'\bar{\phi}_1 \mathrm{d}x - \mathrm{i}v_0v_1 \int_0^1 \phi_2''\bar{\phi}_1 \mathrm{d}x\}}{-\{\mathrm{i}\omega_1 \int_0^1 \phi_1\bar{\phi}_1 \mathrm{d}x + v_0 \int_0^1 \phi_1'\bar{\phi}_1 \mathrm{d}x\}},$$

$$K_3 = \frac{\frac{1}{2}\{-v_1\omega_2 \int_0^1 \phi_1'\bar{\phi}_2 \mathrm{d}x - \frac{v_1\Omega_1}{2} \int_0^1 \phi_1'\bar{\phi}_2 \mathrm{d}x + \mathrm{i}v_0v_1 \int_0^1 \phi_1''\bar{\phi}_2 \mathrm{d}x\}}{-\{\mathrm{i}\omega_2 \int_0^1 \phi_2\bar{\phi}_2 \mathrm{d}x + v_0 \int_0^1 \phi_2'\bar{\phi}_2 \mathrm{d}x\}},$$

$$K_8 = \frac{\frac{v_2}{2}\{\int_0^1 (\omega_2 - \frac{\Omega_2}{2})\bar{\phi}_2'\bar{\phi}_1 \mathrm{d}x + \mathrm{i}v_0 \int_0^1 \bar{\phi}_2''\bar{\phi}_1 \mathrm{d}x\}}{-\{\mathrm{i}\omega_1 \int_0^1 \phi_1\bar{\phi}_1 \mathrm{d}x + v_0 \int_0^1 \phi_1'\bar{\phi}_1 \mathrm{d}x\}}, \quad K_9 = \frac{\frac{v_2}{2}\{\int_0^1 (\omega_1 - \frac{\Omega_2}{2})\bar{\phi}_1'\bar{\phi}_2 \mathrm{d}x + \mathrm{i}v_0 \int_0^1 \bar{\phi}_1''\bar{\phi}_2 \mathrm{d}x\}}{-\{\mathrm{i}\omega_2 \int_0^1 \phi_2\bar{\phi}_2 \mathrm{d}x + v_0 \int_0^1 \phi_2''\bar{\phi}_2 \mathrm{d}x\}},$$

$$s_1 = \frac{\frac{1}{16}v_l^2\{2\int_0^1 \phi_1''\bar{\phi}_1 \mathrm{d}x \int_0^1 \phi_1'\bar{\phi}_1' \mathrm{d}x + \int_0^1 \bar{\phi}_1''\bar{\phi}_1 \mathrm{d}x \int_0^1 \phi_1'^2 \mathrm{d}x\}}{-\{\mathrm{i}\omega_1 \int_0^1 \phi_1\bar{\phi}_1 \mathrm{d}x + v_0 \int_0^1 \phi_1'\bar{\phi}_1 \mathrm{d}x\}},$$

$$s_2 = \frac{\frac{1}{8}v_l^2\{\int_0^1 \bar{\phi}_2''\bar{\phi}_1 \mathrm{d}x \int_0^1 \phi'_1\phi'_2 \mathrm{d}x + \int_0^1 \phi''_1\bar{\phi}_1 \mathrm{d}x \int_0^1 \phi'_2\bar{\phi}_2' \mathrm{d}x + \int_0^1 \phi''_2\bar{\phi}_1 \mathrm{d}x \int_0^1 \phi'_1\bar{\phi}_2' \mathrm{d}x\}}{-\{\mathrm{i}\omega_1 \int_0^1 \phi_1\bar{\phi}_1 \mathrm{d}x + v_0 \int_0^1 \phi'_1\bar{\phi}_1 \mathrm{d}x\}},$$

$$s_3 = \frac{\frac{1}{8}v_l^2\{\int_0^1 \phi''_2\bar{\phi}_2 \mathrm{d}x \int_0^1 \phi'_1\bar{\phi}_1' \mathrm{d}x + \int_0^1 \bar{\phi}_1''\bar{\phi}_2 \mathrm{d}x \int_0^1 \phi'_1\phi'_2 \mathrm{d}x + \int_0^1 \phi''_1\bar{\phi}_2 \mathrm{d}x \int_0^1 \phi'_2\bar{\phi}_2' \mathrm{d}x\}}{-\{\mathrm{i}\omega_2 \int_0^1 \phi_2\bar{\phi}_2 \mathrm{d}x + v_0 \int_0^1 \phi'_2\bar{\phi}_2 \mathrm{d}x\}},$$

$$s_4 = \frac{\frac{1}{16}v_l^2\{2\int_0^1 \phi_2''\bar{\phi}_2 \mathrm{d}x \int_0^1 \phi_2'\bar{\phi}_2' \mathrm{d}x + \int_0^1 \bar{\phi}_2''\bar{\phi}_2 \mathrm{d}x \int_0^1 \phi_2'^2 \mathrm{d}x\}}{-\{\mathrm{i}\omega_2 \int_0^1 \phi_2\bar{\phi}_2 \mathrm{d}x + v_0 \int_0^1 \phi_2'\bar{\phi}_2 \mathrm{d}x\}},$$

$$g_1 = \frac{\frac{1}{16}v_l^2\{2\int_0^1 \bar{\phi}_1''\bar{\phi}_1 \mathrm{d}x \int_0^1 \phi_2'\bar{\phi}_1' \mathrm{d}x + \int_0^1 \phi_2''\bar{\phi}_1 \mathrm{d}x \int_0^1 \bar{\phi}_1'^2 \mathrm{d}x\}}{-\{\mathrm{i}\omega_1 \int_0^1 \phi_1\bar{\phi}_1 \mathrm{d}x + v_0 \int_0^1 \phi_1'\bar{\phi}_1 \mathrm{d}x\}}, \quad g_2 = \frac{\frac{1}{16}v_l^2\{\int_0^1 \phi_1''\bar{\phi}_2 \mathrm{d}x \int_0^1 \phi_1'^2 \mathrm{d}x\}}{-\{\mathrm{i}\omega_2 \int_0^1 \phi_2\bar{\phi}_2 \mathrm{d}x + v_0 \int_0^1 \phi_2'\bar{\phi}_2 \mathrm{d}x\}},$$

$k_{i1} = \mathrm{Im}(K_i),\ k_{i2} = \mathrm{Re}(K_i),\ (i = 2, 3, 8, 9),$

$a_{01} = \mathrm{Re}(s_1),\ a_{02} = \mathrm{Im}(s_1),\ a_{03} = \mathrm{Re}(s_2),\ a_{04} = \mathrm{Im}(s_2), a_{05} = \mathrm{Re}(g_1),\ a_{06} = \mathrm{Im}(g_1),$

$b_{01} = \mathrm{Re}(s_3),\ b_{02} = \mathrm{Im}(s_3),\ b_{03} = \mathrm{Re}(s_4),\ b_{04} = \mathrm{Im}(s_4), b_{05} = \mathrm{Re}(g_2),\ b_{06} = \mathrm{Im}(g_2).$

The nonlinear functions Nf_1^i $(i = 1, 2, 3, 4)$ in (3.20) are

$$\begin{aligned}
Nf_1^1 =& -a_{01}\left(x_1^3 + x_1x_2^2\right) - a_{02}\left(x_1^2x_2 + x_2^3\right) - a_{03}\left(x_1x_3^2 + x_1x_4^2\right) - a_{04}\left(x_2x_3^2 + x_2x_4^2\right)\\
&- a_{05}\left(x_1^2x_3 - x_3x_2^2 + 2x_1x_2x_4\right) + a_{06}\left(2x_1x_2x_3 - x_1^2x_4 + x_2^2x_4\right),\\
Nf_1^2 =& a_{02}\left(x_1^3 + x_1x_2^2\right) - a_{01}\left(x_1^2x_2 + x_2^3\right) - a_{03}\left(x_2x_3^2 + x_2x_4^2\right) + a_{04}\left(x_1x_3^2 + x_1x_4^2\right)\\
&+ a_{05}\left(2x_1x_2x_3 - x_1^2x_4 + x_2^2x_4\right) + a_{06}\left(x_1^2x_3 - x_3x_2^2 + 2x_1x_2x_4\right),\\
Nf_1^3 =& -b_{01}\left(x_1^2x_3 + x_3x_2^2\right) - b_{02}\left(x_1^2x_4 + x_2^2x_4\right) - b_{03}\left(x_3^3 + x_3x_4^2\right) - b_{04}\left(x_4^3 + x_3^2x_4\right) - b_{05}\left(x_1^3 - 3x_1x_2^2\right)\\
&+ b_{06}\left(x_2^3 - 3x_1^2x_2\right),\\
Nf_1^4 =& -b_{01}\left(x_1^2x_4 + x_2^2x_4\right) + b_{02}\left(x_1^2x_3 + x_3x_2^2\right) - b_{03}\left(x_4^3 + x_3^2x_4\right) + b_{04}\left(x_3^3 + x_3x_4^2\right) + b_{05}\left(x_2^3 - 3x_1^2x_2\right)\\
&+ b_{06}\left(x_1^3 - 3x_1x_2^2\right).
\end{aligned}$$

The functions $h_i(\mu_1, \mu_2, \alpha_1, \alpha_2, \beta_1, \beta_2, k_{21}, k_{22}, k_{31}, k_{32}, k_{81}, k_{82}, k_{91}, k_{92})$ $(i = 2, 3, 4)$ in (3.23) are

$$\begin{aligned}
&h_2(\mu_1, \mu_2, \alpha_1, \alpha_2, \beta_1, \beta_2, k_{21}, k_{22}, k_{31}, k_{32}, k_{81}, k_{82}, k_{91}, k_{92})\\
&= -\alpha_1^2 - \alpha_2^2 + \beta_1^2 + \beta_2^2 + 2k_{21}k_{31} - 2k_{22}k_{32} - 2k_{81}k_{91} - 2k_{82}k_{92} + \mu_1^2 + 4\mu_1\mu_2 + \mu_2^2,\\
&h_3(\mu_1, \mu_2, \alpha_1, \alpha_2, \beta_1, \beta_2, k_{21}, k_{22}, k_{31}, k_{32}, k_{81}, k_{82}, k_{91}, k_{92})\\
&= 2\alpha_1^2\mu_2 - 2\alpha_1k_{21}k_{91} + 2\alpha_1k_{22}k_{92} + 2\alpha_1k_{31}k_{81} + 2\alpha_1k_{32}k_{82} + 2\alpha_2^2\mu_2 + 2\alpha_2k_{21}k_{92} + 2\alpha_2k_{22}k_{91}\\
&- 2\alpha_2k_{31}k_{82} + 2\alpha_2k_{32}k_{81} - 2\beta_1^2\mu_2 - 2\beta_1k_{21}k_{32} - 2\beta_1k_{22}k_{31} - 2\beta_1k_{81}k_{92} + 2\beta_1k_{82}k_{91} - 2\beta_2^2\mu_1\\
&- 2\beta_2k_{21}k_{32} - 2\beta_2k_{22}k_{31} + 2\beta_2k_{81}k_{92} - 2\beta_2k_{82}k_{91} - 2k_{21}k_{31}\mu_1 - 2k_{21}k_{31}\mu_2 + 2k_{22}k_{32}\mu_1 + 2k_{22}k_{32}\mu_2\\
&+ 2k_{81}k_{91}\mu_1 + 2k_{81}k_{91}\mu_2 + 2k_{82}k_{92}\mu_1 + 2k_{82}k_{92}\mu_2 - 2\mu_1^2\mu_2 - 2\mu_1\mu_2^2,\\
&h_4(\mu_1, \mu_2, \alpha_1, \alpha_2, \beta_1, \beta_2, k_{21}, k_{22}, k_{31}, k_{32}, k_{81}, k_{82}, k_{91}, k_{92})
\end{aligned}$$

$$
\begin{aligned}
&= -\alpha_1^2\beta_2^2 - \alpha_1^2\mu_2^2 - \alpha_2^2\beta_2^2 - \alpha_2^2\mu_2^2 + \beta_1^2\beta_2^2 + \beta_1^2\mu_2^2 + \beta_2^2\mu_1^2 + k_{21}^2k_{31}^2 + k_{21}^2k_{32}^2 - k_{21}^2k_{91}^2 - k_{21}^2k_{92}^2 + k_{22}^2k_{31}^2\\
&+ k_{22}^2k_{32}^2 - k_{22}^2k_{91}^2 - k_{22}^2k_{92}^2 - k_{31}^2k_{81}^2 - k_{31}^2k_{82}^2 - k_{32}^2k_{81}^2 - k_{32}^2k_{82}^2 + k_{81}^2k_{91}^2 + k_{81}^2k_{92}^2 + k_{82}^2k_{91}^2 + k_{82}^2k_{92}^2\\
&+ \mu_1^2\mu_2^2 + 2\alpha_1\beta_2k_{21}k_{92} + 2\alpha_1\beta_2k_{22}k_{91} + 2\alpha_1\beta_2k_{31}k_{82} - 2\alpha_1\beta_2k_{32}k_{81} + 2\alpha_1k_{21}k_{91}\mu_2 - 2\alpha_1k_{22}k_{92}\mu_2\\
&- 2\alpha_1k_{31}k_{81}\mu_2 - 2\alpha_1k_{32}k_{82}\mu_2 + 2\alpha_2\beta_2k_{21}k_{91} - 2\alpha_2\beta_2k_{22}k_{92}\\
&+ 2\alpha_2\beta_2k_{31}k_{81} + 2\alpha_2\beta_2k_{32}k_{82} - 2\alpha_2k_{21}k_{92}\mu_2 - 2\alpha_2k_{22}k_{91}\mu_2 + 2\alpha_2k_{31}k_{82}\mu_2\\
&- 2\alpha_2k_{32}k_{81}\mu_2 - 2\beta_1\beta_2k_{21}k_{31} + 2\beta_1\beta_2k_{22}k_{32} - 2\beta_1\beta_2k_{81}k_{91} - 2\beta_1\beta_2k_{82}k_{92} + 2\beta_1k_{21}k_{32}\mu_2 + 2\beta_1k_{22}k_{31}\mu_2\\
&+ 2\beta_1k_{81}k_{92}\mu_2 - 2\beta_1k_{82}k_{91}\mu_2 + 2\beta_2k_{21}k_{32}\mu_1 + 2\beta_2k_{22}k_{31}\mu_1 - 2\beta_2k_{81}k_{92}\mu_1 + 2\beta_2k_{82}k_{91}\mu_1 + 2k_{21}k_{31}\mu_1\mu_2\\
&- 2k_{22}k_{32}\mu_1\mu_2 - 2k_{81}k_{91}\mu_1\mu_2 - 2k_{82}k_{92}\mu_1\mu_2.
\end{aligned}
$$

The nonlinear functions $Nf_2^i\,(i = 1, 2, 3, 4)$ in (4.7) are

$$
\begin{aligned}
Nf_2^1 =&\frac{27}{4}z_1^2z_2 + 37z_1^2z_3 - 5z_1^2z_4 - \frac{63}{8}z_1z_2^2 - \frac{651}{4}z_1z_3^2 + 4z_1z_4^2 + \frac{701}{32}z_2^2z_3 - 26z_2^2z_4 + \frac{5619}{64}z_2z_3^2 - \frac{3}{4}z_2z_4^2\\
&- \frac{1261}{16}z_3^2z_4 - 7z_3z_4^2 - 4z_1^3 + \frac{2333}{32}z_2^3 + \frac{4015}{16}z_3^3 - z_4^3 + \frac{63}{2}z_1z_3z_4 - \frac{305}{8}z_1z_2z_3 + \frac{169}{8}z_2z_3z_4\\
&- \frac{3}{2}z_1z_2z_4,\\
Nf_2^2 =&-\frac{23}{13}z_1^2z_2 - \frac{139}{26}z_1^2z_3 + \frac{30}{13}z_1^2z_4 - \frac{123}{52}z_1z_2^2 + \frac{3613}{104}z_1z_3^2 + \frac{6}{13}z_1z_4^2 - \frac{4451}{208}z_2^2z_3 + \frac{17}{52}z_2^2z_4\\
&- \frac{3691}{208}z_2z_3^2 - \frac{29}{13}z_2z_4^2 + \frac{2215}{104}z_3^2z_4 + \frac{35}{26}z_3z_4^2 - \frac{2}{13}z_1^3 - \frac{1403}{52}z_2^3 - \frac{33177}{416}z_3^3 - \frac{10}{13}z_4^3 - \frac{189}{13}z_1z_3z_4\\
&- \frac{17}{26}z_1z_2z_3 - \frac{29}{13}z_2z_3z_4 + \frac{48}{13}z_1z_2z_4,\\
Nf_2^3 =&\frac{2}{13}z_1^2z_2 + \frac{137}{26}z_1^2z_3 - \frac{6}{13}z_1^2z_4 + \frac{87}{52}z_1z_2^2 - \frac{239}{104}z_1z_3^2 + \frac{30}{13}z_1z_4^2 - \frac{7305}{208}z_2^2z_3 + \frac{85}{52}z_2^2z_4 + \frac{5755}{104}z_2z_3^2\\
&+ \frac{50}{13}z_2z_4^2 + \frac{3301}{104}z_3^2z_4 - \frac{241}{26}z_3z_4^2 - \frac{10}{13}z_1^3 + \frac{2805}{104}z_2^3 - \frac{21949}{416}z_3^3 + \frac{2}{13}z_4^3 - \frac{87}{13}z_1z_3z_4 - \frac{62}{13}z_1z_2z_3\\
&- \frac{459}{26}z_2z_3z_4 + \frac{6}{13}z_1z_2z_4,\\
Nf_2^4 =&\frac{27}{4}z_1^2z_2 + \frac{75}{8}z_1^2z_3 - \frac{7}{2}z_1^2z_4 + \frac{491}{16}z_1z_2^2 - \frac{605}{32}z_1z_3^2 + \frac{13}{2}z_1z_4^2 - \frac{3021}{64}z_2^2z_3 - \frac{633}{16}z_2^2z_4 + \frac{287}{64}z_2z_3^2\\
&+ \frac{25}{4}z_2z_4^2 + \frac{1409}{32}z_3^2z_4 - \frac{179}{8}z_3z_4^2 + \frac{1}{2}z_1^3 + \frac{1145}{16}z_2^3 - \frac{8295}{128}z_3^3 - \frac{3}{2}z_4^3 - \frac{11}{4}z_1z_3z_4 + \frac{141}{8}z_1z_2z_3\\
&+ \frac{127}{4}z_2z_3z_4 - 22z_1z_2z_4.
\end{aligned}
$$

The nonlinear functions $Nf_3^i\,(i = 1, 2, 3, 4)$ in (4.32) are

$$
\begin{aligned}
Nf_3^1 =&\frac{5\sqrt{3}}{48}z_2^3 - \frac{\sqrt{3}}{6}z_4^3 - \frac{13}{16}z_1z_2^2 - 2z_1z_4^2 - \frac{55}{4}z_1z_3^2 - \frac{8\sqrt{15}}{3}z_2z_3z_4 - \frac{69}{16}z_1^3 - 2\sqrt{5}z_1z_3z_4 - 2\sqrt{5}z_1z_2z_3\\
&+ 3\sqrt{15}z_1^2z_3 + \frac{3\sqrt{15}}{2}z_3z_4^2 + \frac{\sqrt{15}}{3}z_2^2z_3 + \frac{23\sqrt{3}}{16}z_1^2z_2 - \frac{55\sqrt{3}}{12}z_2z_3^2 - \frac{5\sqrt{3}}{3}z_2z_4^2 + \frac{39\sqrt{3}}{8}z_1^2z_4\\
&+ \frac{7\sqrt{3}}{24}z_2^2z_4 + \frac{35\sqrt{15}}{6}z_3^3 + 10\sqrt{3}z_3^2z_4 - \frac{1}{4}z_1z_2z_4,
\end{aligned}
$$

$$
\begin{aligned}
Nf_3^2 = &-\frac{15\sqrt{3}}{16}z_1^3 - \frac{81}{16}z_1^2z_2 - \frac{65}{4}z_2z_3^2 - 4z_2z_4^2 + \frac{111}{8}z_1^2z_4 + \frac{5}{8}z_2^2z_4 + \frac{25\sqrt{5}}{2}z_3^3 + 60z_3^2z_4 + 6\sqrt{15}z_1z_3z_4 \\
&- 2\sqrt{15}z_1z_2z_3 - \frac{17}{16}z_2^3 + \frac{25}{2}z_4^3 - 4\sqrt{5}z_2z_3z_4 - \frac{19\sqrt{3}}{4}z_1z_2z_4 + 3\sqrt{5}z_1^2z_3 + \frac{25\sqrt{3}}{16}z_1z_2^2 \\
&+ 9\sqrt{3}z_1z_4^2 + \frac{15\sqrt{3}}{4}z_1z_3^2 + \frac{27\sqrt{5}}{2}z_3z_4^2 - \sqrt{5}z_2^2z_3, \\
Nf_3^3 = &\frac{11\sqrt{5}}{120}z_2^3 - \frac{4\sqrt{5}}{3}z_4^3 - \frac{3}{2}z_1^2z_3 - 13z_3z_4^2 - \frac{7}{6}z_2^2z_3 + \frac{13\sqrt{15}}{30}z_1z_2z_4 - \frac{35}{3}z_3^3 + \frac{4\sqrt{3}}{3}z_1z_3z_4 \\
&+ \frac{7\sqrt{3}}{3}z_1z_2z_3 - \frac{17\sqrt{15}}{40}z_1z_2^2 - \frac{13\sqrt{15}}{30}z_1z_4^2 - \frac{2\sqrt{15}}{3}z_1z_3^2 + \frac{\sqrt{5}}{12}z_2^2z_4 + \frac{43\sqrt{5}}{30}z_2z_4^2 + \frac{41\sqrt{5}}{40}z_1^2z_2 \\
&- \frac{5\sqrt{15}}{8}z_1^3 + \frac{21\sqrt{5}}{20}z_1^2z_4 - 5\sqrt{5}z_3^2z_4 + \frac{20}{3}z_2z_3z_4 + \frac{8\sqrt{5}}{3}z_2z_3^2, \\
Nf_3^4 = &\sqrt{3}z_1^3 - 2z_1^2z_2 - \frac{25}{6}z_2z_3^2 - \frac{23}{6}z_2z_4^2 - 3z_1^2z_4 - \frac{7}{3}z_2^2z_4 + \frac{10\sqrt{5}}{3}z_3^3 + 5z_3^2z_4 - \frac{8\sqrt{15}}{3}z_1z_3z_4 \\
&- \frac{2\sqrt{15}}{3}z_1z_2z_3 - \frac{2}{3}z_2^3 - \frac{11}{3}z_4^3 - \frac{4\sqrt{5}}{3}z_2z_3z_4 + \frac{2\sqrt{3}}{3}z_1z_2z_4 + \sqrt{3}z_1z_2^2 - \frac{19\sqrt{3}}{6}z_1z_4^2 - \frac{5\sqrt{3}}{6}z_1z_3^2 \\
&+ 2\sqrt{5}z_3z_4^2 - \frac{2\sqrt{5}}{3}z_2^2z_3.
\end{aligned}
$$

AIMS Press